Assessment Cover

STUDENTS, PLEASE COPY THIS PAGE AND USE AS THE COVER PAGE FOR YOUR SUBMISSION

Module No:	**ENGR7006**	Module title:	**Advanced Vehicle Aerodynamics**

Assessment title:	**CFD Coursework Report**

Due date and time:	13:00hrs Tuesday 20th December 2022, Week 13.

Estimated total time to be spent on assignment:	**60 hours per student**

LEARNING OUTCOMES

On successful completion of this module, students will be able to achieve the module following learning outcomes (LOs): *LO numbers and text copied and pasted from the module descriptor*.
LO 1: Evaluate ground vehicle design features, associated flow structures and vehicle performance characteristics using a range of communication methods.
LO 2: Demonstrate knowledge and understanding of experimental techniques applicable for the evaluation and investigation of aerodynamic performance of ground vehicles through a range of communication methods.
LO 5: Review and critically compare research papers relating to vehicle aerodynamics and present a written report.
LO 6: Develop and implement an appropriate methodology to investigate ground vehicle aerodynamic performance using suitable computational/experimental methods and evaluate the output.
LO 7: Outline the essential requirements concerning the application of CFD to ground vehicle aerodynamic modelling using a range of communication methods.

Engineering Council AHEP4 LOs assessed (from S1 2022-23):	
M1	Apply a comprehensive knowledge of mathematics, statistics, natural science and engineering principles to the solution of complex problems. Much of the knowledge will be at the forefront of the particular subject of study and informed by a critical awareness of new developments and the wider context of engineering
M2	Formulate and analyse complex problems to reach substantiated conclusions. This will involve evaluating available data using first principles of mathematics, statistics, natural science and engineering principles, and using engineering judgment to work with information that may be uncertain or incomplete, discussing the limitations of the techniques employed
M3	Select and apply appropriate computational and analytical techniques to model complex problems, discussing the limitations of the techniques employed
M4	Select and critically evaluate technical literature and other sources of information to solve complex problems
M13	Select and apply appropriate materials, equipment, engineering technologies and processes, recognising their limitations
M16	Function effectively as an individual, and as a member or leader of a team. Evaluate effectiveness of own and team performance

M17	Communicate effectively on complex engineering matters with technical and non-technical audiences, evaluating the effectiveness of the methods used
M18	Plan and record self-learning and development as the foundation for lifelong learning/CPD

STUDENT NAME(S)

Student No:	Student Name:	Group Name and Number:
1. -	-	-

Statement of Compliance *(please tick to sign)*

x	I declare that the work submitted is my own and that the work I submit is fully in accordance with the University regulations regarding assessments

(www.brookes.ac.uk/uniregulations/current)

Effect of Rake in High Yaw Conditions

ABSTRACT

New WRC regulations ban the use of rear diffusers to generate downforce in Rally cars. The solution that many rally teams came up with is using rake, the voerall angle of attack of the vehicle with respect to the ground. In this study, CFD methodology using a simplified bluff body in 3 different rake configurations is used to evaluate the effects of such rake in the aerodynamic performance of the car and the consequences of it when subject to yaw, which is a scenario that rally cars are subject to the majority of the time during stages. It was found that it does not only influence the drag by very little, but rake also increases the downforce generation of the car, whist making the car much more predictable to yawing moment. However, the loss of downforce is steeper on the rake vehicle as yaw is increased.

CONTENTS

1 INTRODUCTION

Rake is the term used to describe the angle between the underbody of a vehicle and the parallel to the ground, which can also be defined as the overall angle of attack of the car with respect to the windspeed, as seen in figure 1. Under normal conditions, it acts as a long diffuser, accelerating the flow under the car and therefore increasing the pressure gradient and the downforce. Due to the new FIA regulations in WRC, cars are no longer authorised to use diffusers, increasing once again the challenge to mitigate the effect of this rule in the car performance. The solutions proposed by the teams, as explained in wrcwings.com (2021), involve the introduction of rake angle, as well as some modifications in the exhaust and hybrid unit cooling systems outlet to help flow acceleration.

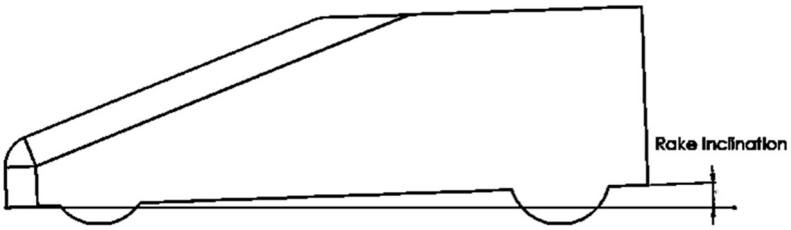

Figure 1. Definition of Rake angle.

The purpose and objectives of this investigation is to acquire firstly, significant figures of the effect of rake and its limitations in terms of performance, and secondly, evaluate the effect of the vehicle lift distribution and its effects on the forces perceived by the vehicle when subjected to yaw, considering the high slip and yaw angles that are experienced by WRC cars during stages.

2 BACKGROUND

Diffusers have been a long-time downforce generation device. They are primordially based in mass flow continuity and Bernoulli's principle, stated in equations 1 and 2.

$$p = p_s + \frac{1}{2}\rho u^2 \, , \rho A u = const. \qquad \textit{eq. 1 \& 2}$$

Applying this to the geometry of figure 2 and rearranging this equation, while assuming incompressibility, since racing speeds are way below compressible flow, we get that:

$$V_1 = V_2 \times (\frac{A_2}{A_1}) \qquad \textit{eq. 3}$$

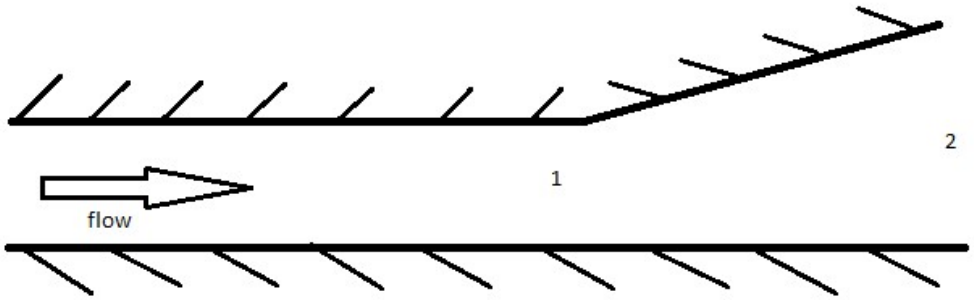

Figure 2. Diffuser geometry for reference in equation 3.

Bernoulli's principle as seen in equation 3 states that when the velocity is higher, the pressure must be lower, which creates a downforce along the underbody of the vehicle. This also has very low drag penalty in comparison to normal downforce generating wings and spoilers, as long as the car front end doesn't show an upwards profile, which will reduce the front wheel down force. (Barnard, 2001)

For high performance, optimum setups will require that the underbody is sealed away from external flows as much as possible, in order to prevent the flow from slowing down, since it will directly affect to the pressure gradient, and therefore the downforce.

When using a diffuser, this problem is solved by extending the side skirts to almost ground level, just as seen in image 4. But as rake is applied, new openings appear that might let side

flow enter the underbody, causing, theoretically, reductions in the pressure gradient generated.

Underbody suction has been used for many years in racing (Singh, 2007), while aerodynamics improvements base themselves in the deviation of external flows from the underbody of the car. As seen in image 3, all car modifications in WRC in the lower part of the car are explicitly design for such purpose. It can be seen that the front of the body is designed to act as a seal by keeping the underbody at a parallel and reasonable low distance from the ground, ensuring a non-upturned nose. Effects of this can also be appreciated in the drag generation of the car, as a front spoiler that seals-off can reduce the drag coefficient in 0.1 (Emmelmann *et. Al,* 2007).

Figure 3. 2022 Hyundai i20 N WRC (Hyundai Motorsport, 2022)

By comparing the 2020 Hyundai i20 Coupe WRC (the year before diffuser ban) in figure 4 and 2022 version of the same car in figure 5, it can be appreciated how the underbody of the 2020 version is completely flat, due to the diffuser presence, and how the 2022 version, with no diffuser, requires a certain level of rake in order to mitigate the effects of the ban in the car performance.

Figure 5. 2022 Hyundai i20 N WRC (Hyundai Motorport, 2022)

Figure 4. 2020 Hyundai i20 Coupe WRC (Hyndai Motorsport, 2020)

3 METHODOLOGY

3.1 TESTING BODY

In 2022, new FIA technical regulations showed that the diffuser is no longer allowed, but a maximum angle of 8° to the reference plane for the rear protection is available to compensate for the loss. (WRC FIA regulations, 2021). The regulations require a flat floor between front and rear wheels, which means a maximum rake angle of 8 degrees is allowed. Ground clearance states that no parts should touch the ground when all 4 tyres are deflated, so using the tyre sidewall as reference (95mm), a ground clearance of 100mm is taken as the distance between the floor and the underbody.

For this work, a bluff body based on the square back version of the Windsor body has been prepared to be simulated (Gaylard *et. Al,* 2017). It will be fitted with dimensions seen in table table 1, which are scaled down to 25% from a normal WRC car. This is a very simplified model designed to study the effects of basic geometry changes, which resembles the overall geometry of a WRC car. It is 1044 mm long, 389 mm high and 289 mm wide; with a stated projected frontal area of 0.112 m2, as seen in figures 6 and 7. Four wheel-like structures were also attached to facilitate the differentiation of Lift forces between front, rear and sides.

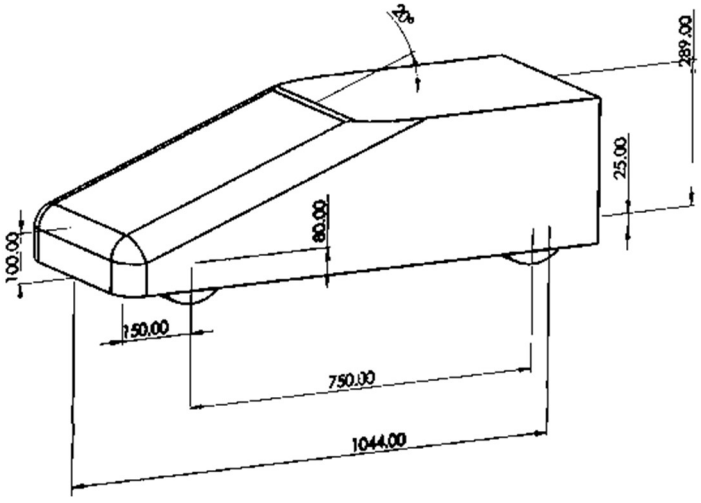

Figure 6. Isometric View of model with dimensions

Dimension	*Units*	*Magnitude*
Length	mm	1044
Front bumper height	mm	100
Height	mm	289
Windscreen inclination	deg	20
Wheelbase	mm	750
Front axle distance from front	mm	150
Tyre centre distance from floor	mm	80
Tyre patch coverage	mm	40
Width	mm	389
Bumper and windscreen fillet radius	mm	50
Wind Tunnel Length	m	10
Wind Tunnel Height	m	2
Wind Tunnel Width	m	2
Front distance to testing section start	m	2.5

Table 1. Numerical Simulations model dimensions

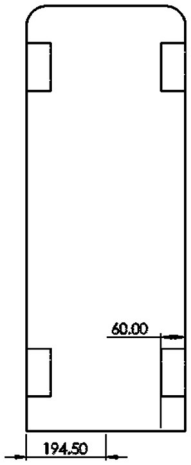

Figure 7. Top View of model with dimensions

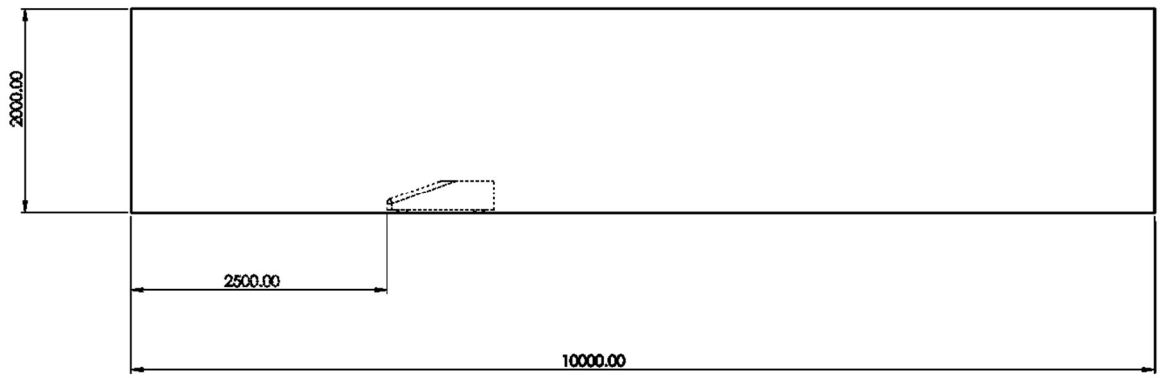

Figure 8. Flow Domain Dimensions

An assumption was made to determine that during stages the sliding angles that WRC cars tend to suffer while maintaining a minimum speed of 30m/s is no more than 45 degrees. Therefore, runs between 0 and 45 degrees in intervals of 9 will be made for rake angles of 0, 2 and 4 degrees. The underbody flow will be compared as well as the lift and drag values with the rolling, yawing and pitching moment induced by aerodynamic forces, in order to find different advantages and disadvantages of such rake angles in the dynamic behaviour of the car.

3.2 COMPUTATIONAL APPROACH

The initial model described above will be created using SOLIDWORKS, while the rest of the Simulation process will be carried out in Star CCM+, postprocessing the results with the help of MATLAB. The flow chart is presented in Figure 9.

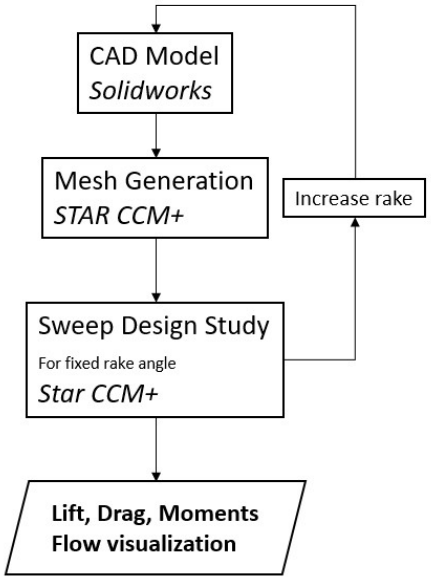

Figure 7. Flow chart of simulations performed

The computer program used to do calculations is Siemens Simcenter Star CCM+, a Multiphysics software that allows for many different types of solvers. We will be using a steady turbulent realizable K-ε model to solve for uncompressible constant velocity. This model suggests a series of modifications that ensure a substantial better performance under boundary layer and separated flows, which is what we primordially will find in the flow round the bluff body, especially under yawed conditions (Hahn, 2007).

For this study, Polyhedral elements with prism layers is the best approach to reduce meshing time. Furthermore, second-moment turbulence RANS simulations are the most cost-effective for flow past ground vehicles (Makowski, 2000). The meshing parameters are described below in table 2. These values ensure for a face validity and volume change sufficiently good to verify the model as suitable, as seen in figure 10.

Parameter	Magnitude	Units
Base cell Size	50	mm
Minimum Size	2.5	%
Target Surface Size	25	%
Surface Growth rate	1.3	%
Custom Outskirts Cell Size	750	%
Prism Layers	2	-
Prism Layer Thickness	33	%

Table 2. Model Mesh parameters

```
-> FACE VALIDITY STATISTICS:
Minimum Face Validity: 1.000000e+00
Maximum Face Validity: 1.000000e+00
        Face Validity <  0.50           0    0.000%
0.50 <= Face Validity <  0.60           0    0.000%
0.60 <= Face Validity <  0.70           0    0.000%
0.70 <= Face Validity <  0.80           0    0.000%
0.80 <= Face Validity <  0.90           0    0.000%
0.90 <= Face Validity <  0.95           0    0.000%
0.95 <= Face Validity <  1.00           0    0.000%
1.00 <= Face Validity              240247   100.000%
-> VOLUME CHANGE STATISTICS:
Minimum Volume Change: 1.106133e-02
Maximum Volume Change: 1.000000e+00
         Volume Change <  0.000000e+00           0    0.000%
0.000000e+00 <= Volume Change <  1.000000e-06           0    0.000%
1.000000e-06 <= Volume Change <  1.000000e-05           0    0.000%
1.000000e-05 <= Volume Change <  1.000000e-04           0    0.000%
1.000000e-04 <= Volume Change <  1.000000e-03           0    0.000%
1.000000e-03 <= Volume Change <  1.000000e-02           0    0.000%
1.000000e-02 <= Volume Change <  1.000000e-01        7202    2.998%
1.000000e-01 <= Volume Change <= 1.000000e+00      233045   97.002%
```

Figure 8. Mesh diagnosis of the model described

The configuration used for the physics model is presented in table 3.

Models	Parameters	Magnitude	Units
Constant density	Pressure	10	KPa
Coupled	Turbulence Intensity	2	%
Steady	Turbulence Length scale	0.01	m
K-ε, All Y+	Velocity	30	m/s

Table 3. Physics Model parameters

It is important to mention, that according to various sources (Basara *et al., 2007)* , current computational methods tend to overestimate drag levels due to the empirical assumptions made by the RANS simulations, while vorticity, wake flow and the rest of force coefficients tend to follow experimental values quite closely. Furthermore, we are neglecting the flow around rotating wheels, which translates to a lift and drag reduction (Wäschle, 2007).However, since this study is not focused on drag reduction, but an observation fo the evolution of the aerodynamic forcers through a range of geometric paramters, this study should output the values of interestfor a sufficient discussion. (Williams *et al.,* 1997).

All forces and moments will be non-dimensioned by suing the reference cross sectional area A_{ref}, wheelbase L and dynamic pressure $q_o = \frac{1}{2}\rho V_\infty^2$. Moments are calculated at the centre of the body, giving force coefficients as follow in equations 3 and 4.

$$F.Coef. = \frac{Force}{q_o \times A_{ref}} \quad \textit{eq. 4}$$

$$M.Coef = \frac{Moment}{q_o \times A_{ref} \times L} \quad \textit{eq. 5}$$

4 DISCUSSION

Results for the lift show that in all 3 configurations there is a tendency to increase the lift as yaw increases. Figure 11 shows the variation of total vehicle lift coefficient. It can be appreciated that this loss is smaller as rake is increased. Furthermore, we can see that Rake introduces a downforce factor, and that it is dependent on the rake angle. It is seen that the angle at which the car transitions from downforce to lift during yaw is higher as we increase the rake. It was expected to generate more downforce as rake angle is increased, following the explanation in the background section.

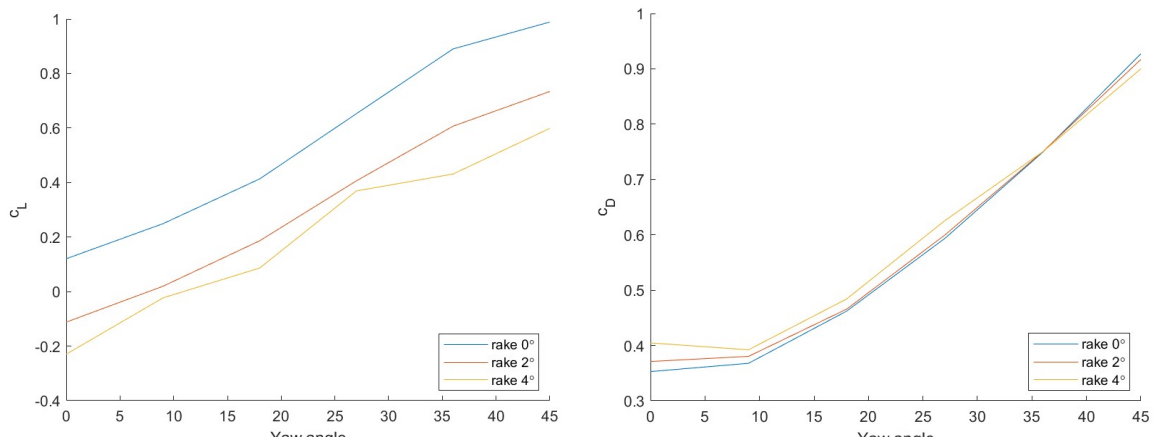

Figure 9. Lift and Drag Coefficient values obtained from CFD along different Rake and Yaw angles

If we focus on the drag, it shows that there is a slight drag increase at small yaw angles as the rake is increased. However, higher rake angles reduce the drag at high yaw ever so slightly. It makes sense for the drag to be higher as the cross-sectional front area is slightly increased with the increase of Rake. Furthermore, this cross-sectional area enlarges as the vehicle yaw is increased, which is translated to an increment in drag.

Results previously obtained by Gilmineau and Chometon confirm this behaviour (Gilmineau, 2007).

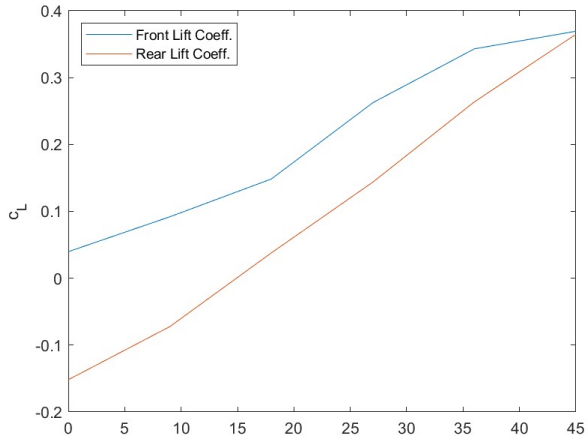

Figure 11. Lift and Rear Lift coefficients for 2 degrees of Rake comparison along the yaw sweep

Figure 13 shows the comparison between Front and Rear lift coefficients for a 2-degree rake. It can be seen that rear lift has increases more rapidly as we sweep along the yaw angles compared to the front lift. This suggest that the centre of pressure is moved towards the rear of the vehicle. This behaviour is examined by Dominy, in whose study the centre of pressure is moved rearwards. (Dominy, 2004)

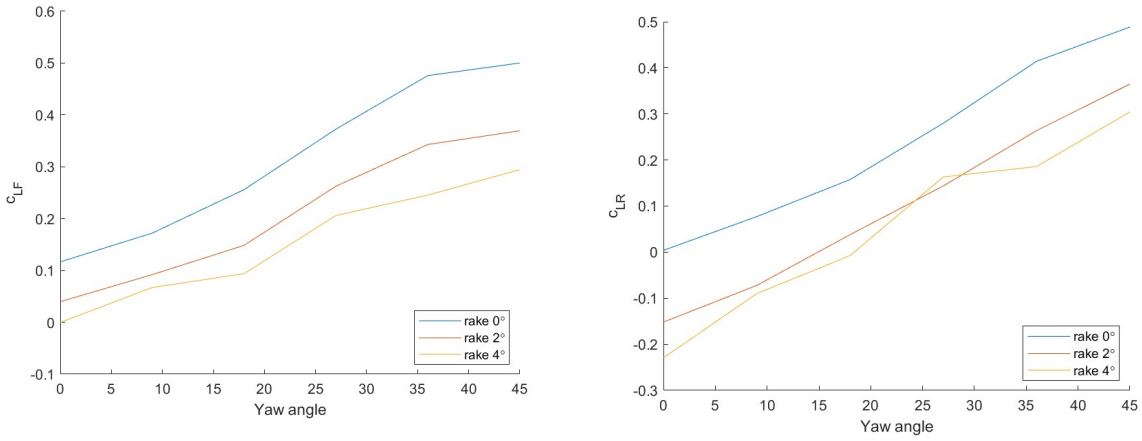

Figure 10. Axle Lift values obtained from CFD along different Rake and Yaw angles.

It can also be seen that this variation also depends on the rake, which tends to follow the same variation profile at the front (since ride height does not vary here), but we start to see some interesting variation when looking at the rear lift coefficient change, looking at figure 12. This variation could be due to the air openings and the slope variation of the sideskirt section of the geometry, which reacts differently as yaw is increase and generates bigger wake regions that travel along the rear section of the underbody, and off to the back of the vehicle.

Figure 14 and 15 show such vortices at 0 and 4 degrees of rake. It is very clear that the wake generated by the rear wheels is very accentuated by the rake variation.

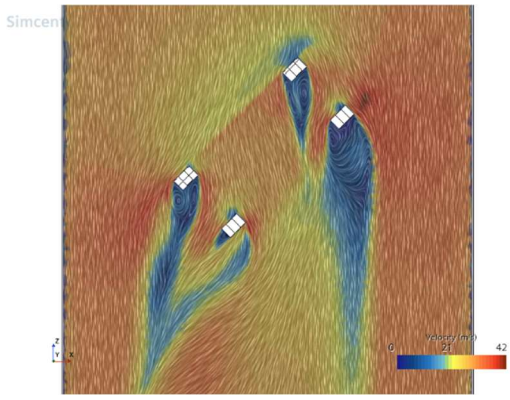

Figure 14. Unederbody Flow visualization with velocity sensibility for the 0 degees of rake configuration at 45 degrees of yaw.

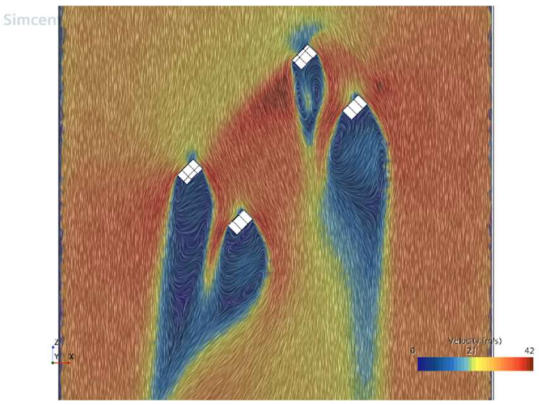

Figure 13. Underbody Flow visualization with velocity sensibility for the 4 degees of rake configuration at 45 degrees of yaw.

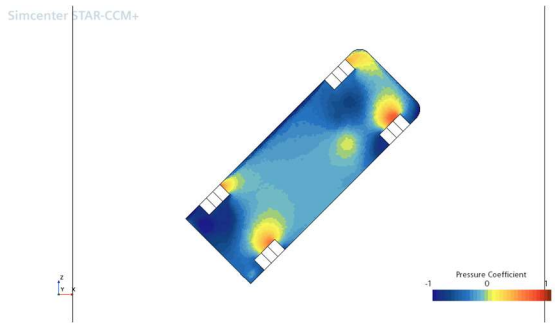

Figure 12. Underbody Pressure Coefficients for the 0 degees of rake configuration at 45 degrees of yaw.

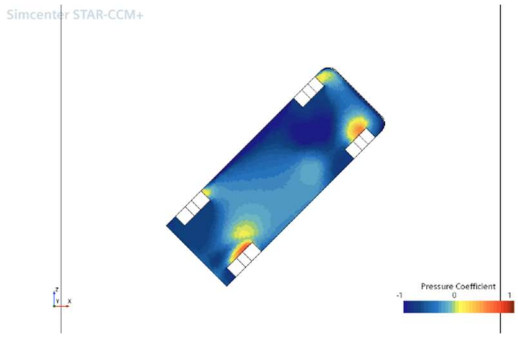

Figure 15. Underbody Pressure Coefficients for the 4 degees of rake configuration at 45 degrees of yaw.

Looking at the pressures for the same configurations in figures 16 and 17, the higher rake angle shows a higher concentration of the pressure towards the rear area. Taking a look at the small pressure concentration see slightly rearwards in the zero rake image, it can be seen that this is shifted towards almost the rear axle in the four degrees rake configuration of the model. Which explains the rearwards movement of the centre of pressure.

If we compare these last images with their alternatives at 0 degrees of yaw in figures 18 and 19, we can see that this pressure increase is also present but the suction pressure obtained at the front axle is much stronger when comparing the rake model with the non-rake one, which explains the downforce gain from one another, and confirms the theory explained in the background section.

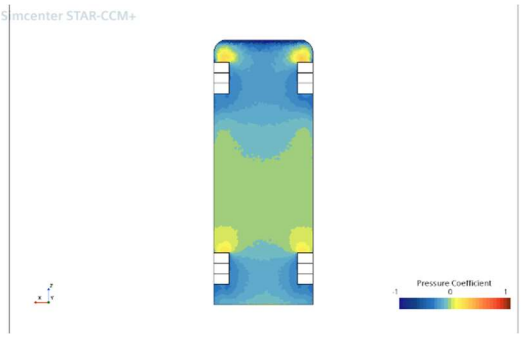

Figure 17. Underbody Pressure Coefficients for the 0 degees of rake configuration at 0 degrees of yaw.

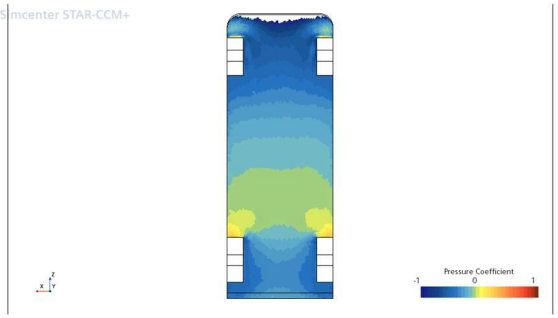

Figure 16. Underbody Pressure Coefficients for the 4 degees of rake configuration at 0 degrees of yaw.

As a consequence of such imbalance between the front and rear lifts caused by yaw angle, pitching moment is also affected, as seen in figure 20. It reduces the nose up pitching moment originally present at 0 degrees of yaw. This reduction is more accentuated at high rake, where the 0-yaw pitching moment is almost double when comparing the zero to the four degrees rake; but all 3 rake configurations tend to converge towards the same range of values at high yaw angles, which is close to 0.

Other investigations carried by Dominy demonstrate that downforce at the front is reduced and the car is more prone to pitch upwards when in yaw.

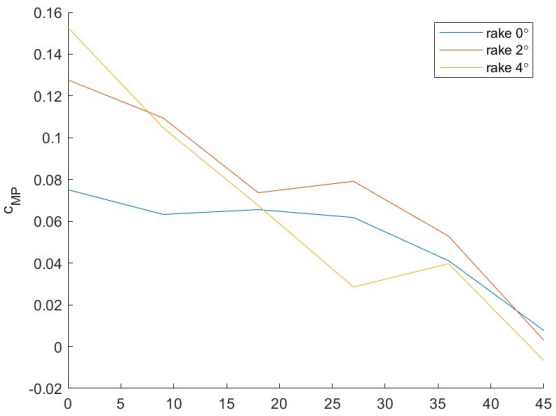

Figure 18. Pitching Moment values obtained from CFD along different Rake and Yaw angles.

However, in this case we find ourselves in the contrary scenario, where the vehicle is more prone to reduce this nose up moment. This is explained by comparing both geometries: whilst the study by Dominy uses a downforce generating car by itself, our vehicle is a simplified shape that generates lift. (Dominy, 2004)

An important aspect to mention, taking a look into table 4, from 0 to 4 degrees of rake, the whole aerodynamic forces are being transferred from front to rear. This certainly contributes to the pitching moment variation from expected results from other studies.

Rake	Pitch Moment	Front Lift	Rear Lift	Total Lift
Degrees	Newtons-meter	Newtons	Newtons	Newtons
0	3.46496	7.1729	0.242973	7.41587
2	6.6094	2.74474	-10.4741	-7.72933
4	8.75732	-0.0140101	-17.5286	-17.5427

Table 4. . Front, rear and total Lift variations along with pitching moment for all rake angles at 0 yaw.

Pitching moments were even reversed in sign when the vehicle was subject to maximum yaw angles, transforming its nature from nose up to nose down.

Rolling moment, shown in figure 21, is also increased, inducing instability to the vehicle when subject to high slips, accentuated at high rake, confirming that the flow channels at the side skirts of the vehicle close to the rear wheel will indeed increase drastically the rolling tendency of the vehicle when cornering at very high slip angles.

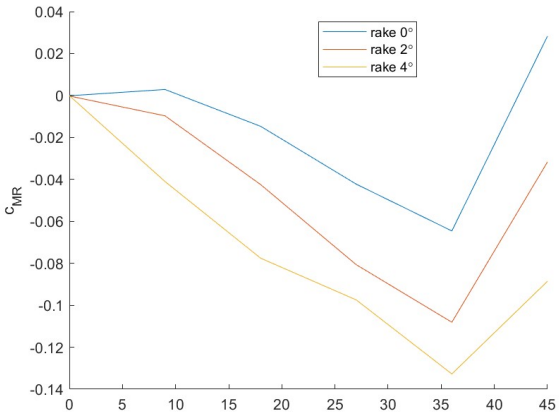

Figure 19. Rolling Moments values obtained from CFD along different Rake and Yaw angles.

Finally, yaw moment is also highly increased towards the wind direction up until 25 degrees when in 0 rake, point from which the yaw moment changes sign and tends to realign the car with the flow direction, as seen in figure 22. This effect is also mitigated at higher rake angles, whilst the critical angle at which the yaw moment changes sign is also decreased. This is due to the increased cross-sectional side area of the vehicle at the rear when compared to the front, which induces a self-aligning moment. This is attributed to the geometry of the vehicle and is subject to the position of the centre of mass.

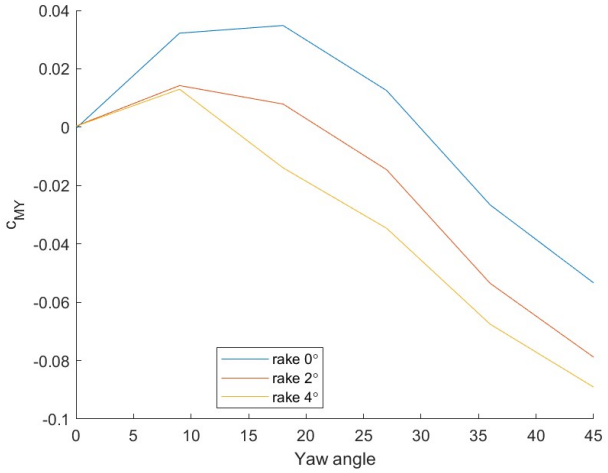

Figure 20. Yawing Moment values obtained from CFD along different Rake and Yaw angles.

A complete tabulation of the results is available in Apendix A.

5 CONCLUSIONS

It has been demonstrated that the vehicle is capable of producing downforce without a diffuser by simply introducing a rake angle; more concisely, the car shifts from developing lift to being having the same magnitude of downforce by simply introducing 2 degrees of rake. It has also been shown that the yawing moment becomes much more predictable as it reduces the variation between small and high yaw angles; meaning that the driver will only be expecting to counter steer into only one direction without depending on the yaw angle that the vehicle is undertaken when cornering.

On the other side, higher rake angles do induce a rolling moment caused by the inflow of air into the side skirt area of the windward side at yaw. Furthermore, if we compare the findings on a downforce generating car to the shape studied in this project, lift forces are increased whatsoever and pitching moments are prone to be balanced when subjecting the car to yaw. This means that, depending on the initial (0 yaw) conditions of the vehicle, its performance will be reduced as a consequence of downforce loss, and an adverse pitching moment will be produced; or it can be possible that its pitching moment is balanced in a positive way, stabilising the vehicle ever so slightly.

6 EXPERIMENTAL VALIDATION

The experimental validation of this conducted CFD investigation is planned to be done in the University of Southampton R J Mitchell Wind Tunnel, used for vehicle aerodynamic works and performance sport testing.

The Wind tunnel is a 3.5 by 2.4 by 10.5 meters working sections with speeds of up to 40 meters per second with a 0.2% turbulence. It also features a 6-component overhead balance, capable of producing any yaw angle and a moving ground. Suitable models for the wind tunnel are 50% maximum scale, which means this tunnel features all facilities needed to validate the 25% scaled model of this project. (University of Southampton, n.d.)

Using the equipment mentioned above, 3 different car models will be constructed with the 3 different rake angles described in the methodology. Each of the models will be run for the 6 different yaw angles. Post processing will require measurements of the real wind speed, pressure and density of the air at the given time of the experiment, in order to obtain force coefficients that can be normalized properly. The model will be mounted from the top, and equipped with rubber mimic wheels that will most likely degrade in the runs, as an effect of the moving ground of the wind tunnel.

In terms of flow visualization, either smoke or paint can be sued, since it is a rather qualitative measure, that lets us understand flow rather than quantize it.

Experimental measures for all scaled models are subject to Reynolds number effect, which states that for all mreasurements to correlate between normal size and scaled models, the flow reynolds number must be equal, following equatuion 6.

$$\frac{\rho V l}{\mu}_{scaled} = \frac{\rho V l}{\mu}_{ful\ \ size} \qquad \textit{eq. 6}$$

Which potentially translates to increasing the flow velocity, as density and viscosity of air remain fixed. However, for this study, no such correction is needed, as the model used for CFD can be reproduced with the exact same dimensions and still fit inside of the wind tunnel selected. Even the wake region used in the numerical simulations stays within the range of the wind tunnel dimensions.

Other correction factors such as blockage effects and rotating wheel neglection are also factors that can led up to no correlations between experimental and numerical values. On the other hand, this study and model geometry are simplistic enough to be able to neglect all this factors, as we are investigating an overview of the response of a body to rake, not an specific sitation of a certain car model, in which case all mentioned factors will need consideration, and a more accurate numerical model based on the selected vehicle dimensions would be used for calculations. Once again, it is not the case of this study.

7 PERSONAL REFLECTION

During the development of this work, I have noticed how much detail needs to be taken into account in the modelling and meshing part of a CFD Study. In this case, the studied areas did not require high level of detaio, however the study can be easily improved by using moving wheels, which will require a refinement of the model and the parts, and even steering modeling can also be taken into account. This study is also focused to Rally cars, in which aerodynamic devices play high role in the performance of the car, and none of them have bee considered. This means that the results obtained for a simple bluff body might be different

when the geometry is applied to higher detail WRC cars. However, this is a simple general overview type of study, rather than a refined optimisiation.

8 REFERENCES

Barnard, R. H. (2001) 'Road Vehicle Aerodynamic Design' 2nd edn. Hertfordshire: Mechaero Publishing.

Basara, B., Aldudak, F., Jakirlic, S., Tropea, C., Schrefl, M., Mayer, J., Hanjalic, K. (2007) 'Experimental Investigations and Computations of Unsteady Flow Past a Real Car Using a Robust Elliptic Relaxation Closure with a Universal Wall Treatment'. *SAE Technical Paper Series 2007-01-0104.*

Emmelmann, H-J., Berneburg, H., Schulze, J. (2007) 'The Aerodynamic Development of the Opel Calibra'. *SAE Technical Paper Series 900317.*

F.J. Bello-Millán *et al.* (2016) 'Experimental study on Ahmed's body drag coefficient for different yaw angles', *Journal of Wind Engineering and Industrial Aerodynamics,* Volume 157, pp. 140-144. Available at: https://doi.org/10.1016/j.jweia.2016.08.005.

FIA (2021) 'Specific regulations for Rally1 Cars'. Appendix J – Article 262. Available at: https://www.fia.com/sites/default/files/262_2022_wmsc_2021.12.15.pdf

Gaylard, A.P., Kabanovs, A., Jilesen, J., Kirwan, K., Lockerby, D.A. (2017) 'Simulation of rear surface contamination for a simple bluff body', *Journal of Wind Engineering and Industrial Aerodynamics,* 165. pp: 13-22. Available at: https://doi.org/10.1016/j.jweia.2017.02.019.

Guilmineau, E., Chometon, F. (2007) 'Experimental and Numerical Analysis of the Effect of Side Wind on a Simplified Car Model', *SAE Technical Paper Series 2007-01-0108.*

Hahn, S.A., Kruse, N., Werner, F. (2007) 'Virtual Aerodynamic Engineering at GM Europe Development of the 2006 OPEL Corsa', *SAE Technical Paper Series 2007-01-0102.*

Hucho, W., Sovran, G. (1993) 'Aerodynamics of road vehicles' in V. Sumantran and G. Sovran *Vehicle Aerodynamics.* Warrendale, PA. Society of Automotive Engineers. pp. 3-60.

Hyundai Motorsport. (2022 Hyundai i20 N WRC Rally1. Available at: https://motorsport.hyundai.com/rally/wrc/i20-n-wrc-rally1/

Hyundai Motorsport. (2022) Hyundai i20 Coupe WRC. Available at: https://motorsport.hyundai.com/rally/wrc/evolution/

Makowski, F.T., Kim, S.E. (2000) 'Advances in External-Aero Simulation of Ground Vehicles Using the Steady RANS Equations' *SAE Technical Paper Series 2000-01-0484.* Available at: https://doi-org.oxfordbrookes.idm.oclc.org/10.4271/2000-01-0484

R. G. Dominy and S. Richardson (2004) 'The Aerodynamic Characteristics of a WRC Rally Car at High Slip Angles', *SAE Technical Paper Series 2004-01-3508.* Available at: https://doi-org.oxfordbrookes.idm.oclc.org/10.4271/2004-01-3508

Singh, R., Shen, F. (2007) 'CFD-based Robust optimization of Front-end Cooling Airflow', *SAE Technical Paper Series 2007-01-0105*.

University of Southampton (2022) *Wind tunnel: 3.5m by 2.4m by 10.5m.* Available at: https://www.southampton.ac.uk/research/facilities/large-wind-tunnel-3.5m-by-2.4m-by-10.5m (Accessed: 11 December 2022)

Wäschle, A. (2007) 'The Influence of Rotating Wheels on Vehicle Aerodynamics – Numerical And Experimental Investigations'. *SAE Technical Paper Series 2007-01-0107.*

Williams, J., Quinlan, W. J., Hackett, J. E., Thompson, S. A., Marinaccio, T., Robertson, A. (1994) 'A Calibration Study of CFD for Automotive Shapes and CD', *SAE Technical Paper Series 940323*

WRCWings (2021) *Toyota proposal for rear diffuser replacement in the 2022 Rally1 hybrid car*. Available at: https://www.wrcwings.tech/2021/09/07/toyota-proposal-for-rear-diffuser-replacement-in-the-2022-rally1-hybrid-car/ (Accessed: 03 November 2022)

Yamada, A., Ito, S. (1996) 'Computational Analysis of Flow Around a Simplified Vehicle-Like Body'. *SAE Technical Paper Series 930293.*

9 APPENDIX A

ID	Rake angle	Yaw angle	Drag	Total Lift	Front Lift	Rear Lift	Frontal Area	Pitch Moment	Roll Moment	Yaw moment
	Degrees	Degrees	Newtons	Newtons	Newtons	Newtons	Meters^2	Newtons-meter	Newtons-meter	Newtons-meter
1	0	0	-21.705	7.416	7.173	0.243	0.115	3.465	-0.003	-0.019
2	0	9	-30.127	20.400	14.087	6.314	0.154	3.887	0.091	1.978
3	0	18	-46.008	41.143	25.469	15.674	0.187	4.898	-0.569	2.600
4	0	27	-68.120	74.905	42.776	32.129	0.215	5.323	-1.887	1.080
5	0	36	-96.476	114.586	61.262	53.324	0.242	3.969	-3.233	-2.570
6	0	45	-128.947	137.503	69.559	67.944	0.261	0.807	1.530	-5.566
7	2	0	-25.615	-7.729	2.745	-10.474	0.130	6.609	-0.007	0.020
8	2	9	-34.395	1.777	8.311	-6.534	0.170	7.422	-0.341	0.966
9	2	18	-50.395	20.162	16.060	4.102	0.203	5.979	-1.787	0.642
10	2	27	-74.078	50.199	32.436	17.763	0.232	7.336	-3.877	-1.350
11	2	36	-103.469	83.663	47.298	36.365	0.259	5.467	-5.798	-5.533
12	2	45	-135.861	108.762	54.721	54.041	0.278	0.340	-1.826	-8.757
13	4	0	-30.942	-17.543	-0.014	-17.529	0.143	8.757	-0.002	0.018
14	4	9	-38.792	-2.281	6.630	-8.911	0.186	7.770	-1.578	0.964
15	4	18	-56.593	10.109	10.975	-0.866	0.219	5.921	-3.526	-1.222
16	4	27	-82.849	48.895	27.282	21.613	0.249	2.835	-5.020	-3.441
17	4	36	-110.498	63.526	36.151	27.375	0.276	4.388	-7.605	-7.456
18	4	45	-141.835	94.358	46.395	47.963	0.296	-0.784	-5.429	-10.527